DETECTION OF HCN DIRECT *l*-TYPE TRANSITIONS PROBING HOT MOLECULAR GAS IN THE PROTO–PLANETARY NEBULA CRL 618

S. THORWIRTH,[1] F. WYROWSKI,[2,3] P. SCHILKE,[3] K. M. MENTEN,[3] S. BRÜNKEN,[1]
H. S. P. MÜLLER,[1] AND G. WINNEWISSER[1]

ABSTRACT

We report the detection of direct *l*-type transitions toward the proto–planetary nebula CRL 618 during a study of vibrationally excited carbon chains. The $J = 8$, 10, 11, 12, 13, and 14 $\Delta J = 0$ transitions of HCN in its first excited bending mode $v_2 = 1$ were detected in absorption against the continuum of the central H II region, making use of the Effelsberg 100 m telescope and the Very Large Array. In addition, the $J = 9$ direct *l*-type transition was detected in emission, presumably indicating a weak maser. All lines are blueshifted with respect to the systemic velocity of CRL 618, indicating that the lines originate from a hot, expanding circumstellar envelope. The HCN column density along the line of sight in front of the continuum is 2×10^{18} cm^{-2}.

Subject headings: line: identification — radiation mechanisms: nonthermal — radio lines: stars — stars: AGB and post-AGB — stars: individual (CRL 618) — stars: mass loss

1. INTRODUCTION

Molecules in vibrationally excited states are unique tools for studying hot molecular gas in interstellar and circumstellar environments. The vibrationally excited states can be pumped by IR radiation in the dusty environment close to the exciting object (see, e.g., Schilke et al. 1992; Schilke, Mehringer, & Menten 2000; Wyrowski, Schilke, & Walmsley 1999 and references therein).

A linear molecule with N atoms has $3N - 5$ vibrational modes. For HCN, this yields four vibrational modes,[4] two of which are stretching modes (CN stretch ν_1, CH stretch ν_3), and the H—C—N bending mode (ν_2), which is doubly degenerate since the molecule is free to bend in two orthogonal planes. If the molecule is bending and rotating simultaneously, the degeneracy is lifted, giving rise to a phenomenon denoted *l-type doubling*: the degenerate bending state can be regarded as having components of an additional angular momentum $p = l\hbar$ about the figure axis, with $l = v$, $v - 2$, $v - 4$, ..., $-v$. For a first excited bending mode, $l = +1$, -1 causes the splitting of every rotational level into two sublevels. Now two different types of transitions with either $\Delta J = \pm 1$ or $\Delta J = 0$ may occur, the latter being denoted *direct l-type transitions* (see Fig. 1). Since the splitting of the sublevels of a given J is rather small, the corresponding transitions occur at low frequencies. For a molecule in a first excited bending mode, these are to first order given by $\nu = qJ(J + 1)$, where q is the *l*-type doubling constant ($q_{(HCN, v_2=1)} \approx 224$ MHz).

In the laboratory, direct *l*-type transitions were first measured by Shulman & Townes (1950) for the molecules HCN and OCS. In space, rotational transitions of vibrationally excited HCN ($\Delta J = \pm 1$, $v_2 = 1$, 2; "vibrational satellites") were first detected by Ziurys & Turner (1986) toward Orion KL and IRC +10216. Meanwhile, HCN was also detected in much higher vibrationally excited states (e.g., $v_2 = 4$; Schilke et al. 2000; Schilke & Menten 2003). A detection of the $J = 19$ direct *l*-type transition of HCN ($v_2 = 1$) in IRC +10216 was previously reported by Cernicharo et al. (1996), although no details were given.

We started a detailed study of vibrationally excited carbon chain molecules toward the proto–planetary nebula CRL 618 at radio and millimeter wavelengths to examine their radial distribution by measuring their vibrational temperatures. In this paper, we report the first detection of seven consecutive direct *l*-type transitions of HCN ($v_2 = 1$) at centimeter wavelengths, from $J = 8$ through 14. The results on the higher cyanopolyynes HC$_3$N and HC$_5$N are reported separately (Wyrowski et al. 2003; Thorwirth 2001).

2. OBSERVATIONS

2.1. *Effelsberg 100 m Observations*

The observations were performed during eight observing sessions from 1999 March to 2002 January employing the 100 m radio telescope of the Max-Planck-Institut für Radioastronomie at Effelsberg, Germany. As front ends, the 0.65, 1, 1.3, and 1.9 cm HEMT receivers with typical receiver temperatures from 30 to 70 K, respectively, were used. The FWHM beam widths and the frequencies of the HCN lines are given in Table 1. Pointing was checked every 1–2 hr on CRL 618 itself or other appropriate radio sources, resulting in an average pointing accuracy of 4″. The intensity scale was established using continuum drift scans on W3(OH), NGC 7027, and 3C 147 and comparing with the flux densities given by Ott et al. (1994). Pointing scans on CRL 618 were used to determine its flux density relative to these calibration sources (Table 1).

[1] I. Physikalisches Institut, Universität zu Köln, Zülpicher Strasse 77, 50937 Cologne, Germany; sven@ph1.uni-koeln.de, bruenken@ph1.uni-koeln.de, hspm@ph1.uni-koeln.de, winnewisser@ph1.uni-koeln.de.

[2] Department of Astronomy, University of Maryland, College Park, MD 20742-2421.

[3] Max-Planck-Institut für Radioastronomie, Auf dem Hügel 69, 53121 Bonn, Germany; wyrowski@mpifr-bonn.mpg.de, schilke@mpifr-bonn.mpg.de, kmenten@mpifr-bonn.mpg.de.

[4] For the sake of clarity it should be recalled that ν is used to denote a certain vibrational mode or the frequency, whereas v denotes the vibrational quantum number.
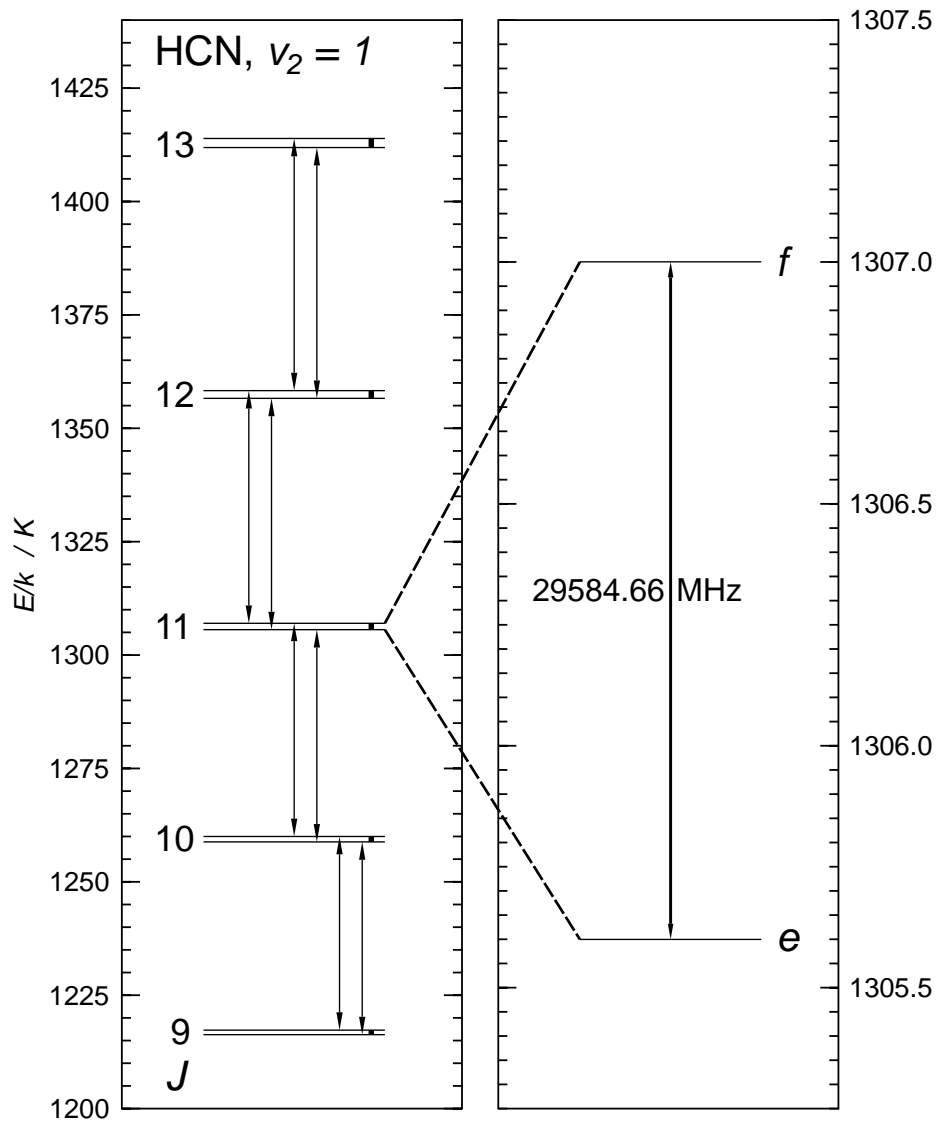
FIG. 1.—Term value diagram of HCN in its $v_2 = 1$ vibrational state from $J = 9$ to $J = 13$. On the left-hand side both possible types of transitions with $\Delta J = \pm 1$ and the direct l-type transitions with $\Delta J = 0$ are shown. The diagram on the right-hand side shows the $J = 11$ direct l-type transition at 29,584.66 MHz in detail. According to the convention of Brown et al. (1975), the vibrational substates have been labeled e (lower) and f (upper).

TABLE 1
DIRECT l-TYPE TRANSITIONS OF HCN

J	Frequency[a]	E_u	θ_{mb}	$-T_L/T_C$	I_L	v_L	Δv	S_ν^{cont}
4...............	4488.48	1067		[b]				26 (3)
8...............	16148.55	1178	52	[c]		−26.6 (3)	3.8 (5)	
9...............	20181.40	1217	42		22 (4)	−27.0 (3)	4.7 (7)	425 (60)
10..............	24660.31	1259	34	0.11 (3)		−26.6 (3)	4.4 (6)	490 (90)
11..............	29584.66	1307	28	0.05 (1)		−27.0 (2)	4.8 (6)	[d]
12..............	34953.76	1358	24	0.07 (2)		−27.4 (2)	5.1 (4)	680 (140)
13..............	40766.90	1413	0.33	0.11 (4)		−27.3 (7)	5.4 (12)	750 (75)
14..............	47023.20	1473	20	0.11 (4)		−26.7 (4)	4.9 (11)	840 (85)

NOTES.—Shown are the direct l-type transitions of HCN (MHz) in its $v_2 = 1$ vibrational state observed in the present study, as well as corresponding upper energies (K), beam sizes θ_{mb} (arcsec), line-to-continuum ratios, line intensities I_L (mJy), line velocities v_L (km s^{-1}), line widths Δv (km s^{-1}), and continuum flux densities S_ν^{cont} (mJy).

[a] Laboratory frequencies taken from Maki 1974.
[b] No line detected.
[c] Line detected in absorption without valid calibration.
[d] No absolute flux calibrator available.

2.2. *CSO Observations*

Spectra of the $J = 4$–3 line of HCN in its ν_2 bending mode were obtained in 1999 December with the 10.4 m telescope of the Caltech Submillimeter Observatory (CSO)[5] with a system temperature of 600 K. The line was observed in the upper sideband, and several different observing frequencies were used to avoid blending from lines in the lower sideband. The spectrometer and observing procedure are described by Menten & Young (1995). The CSO beam size at 356 GHz is $26''$, and we assumed a beam efficiency of 78% (taken from the CSO Web site).

2.3. *VLA Observations*

CRL 618 was observed in the $J = 13$ direct l-type transition (see Table 1) with the Very Large Array (VLA)[6] in its B configuration, leading to an angular resolution of $0''\!.12$. At the time of the observations, 15 antennas were equipped with 0.7 cm receivers. A total bandwidth of 6.25 MHz was observed with 128 channels, and the spectral resolution was 48.8 kHz. The total time on source was 3.5 hr. Regular observations of 0555+398, 3C 48, and 3C 84 were used for amplitude, flux, and bandpass calibration, respectively. The phase was self-calibrated on the strong continuum emission from CRL 618.

The remaining non–Q-band antennas were used to observe the $J = 4$ direct l-type transition at 4488.48 MHz. No line was detected at an rms noise level of 4 mJy in 0.8 km s^{-1} wide channels. The total continuum flux at this frequency is 26 ± 3 mJy.

3. RESULTS AND DISCUSSION

Figure 2 shows the direct l-type lines observed toward CRL 618, and the line parameters from Gaussian fits to the spectra are given in Table 1. The $J = 8$, 10, 11, 12, 13, and 14 direct l-type transitions appear as absorption lines toward the continuum of the H II region, with line velocities of approximately $v_L = -27$ km s^{-1}. The systemic velocity v_{sys} of CRL 618 is -24.2 km s^{-1} (Wyrowski et al. 2003); hence, all of the observed lines are blueshifed relative to v_{sys}, indicating that the lines originate from a hot, expanding circumstellar envelope. To determine the physical conditions of the absorbing gas, we used a spherical LTE model of an expanding envelope, developed to interpret our observations of vibrationally excited HC$_3$N derived by Wyrowski et al. (2003). To fit the HCN lines we use the temperature, density, and velocity structure of the expanding envelope, which fitted the HC$_3$N lines, and vary only the HCN abundance. Using a temperature of 560 K (see discussion below), an HCN column density of 2×10^{18} cm^{-2} is needed to cause the observed absorption. The resulting fits to the spectra are shown in Figure 3, together with a spectrum of the HC$_3$N $v_4 = 1$ $J = 12$–11 transition, which has a similar upper energy ($\sim$1300 K). Since no continuum flux measurements were performed at 350 GHz, the HCN $J = 4$–3 spectra are shown in brightness temperature units, whereas for the
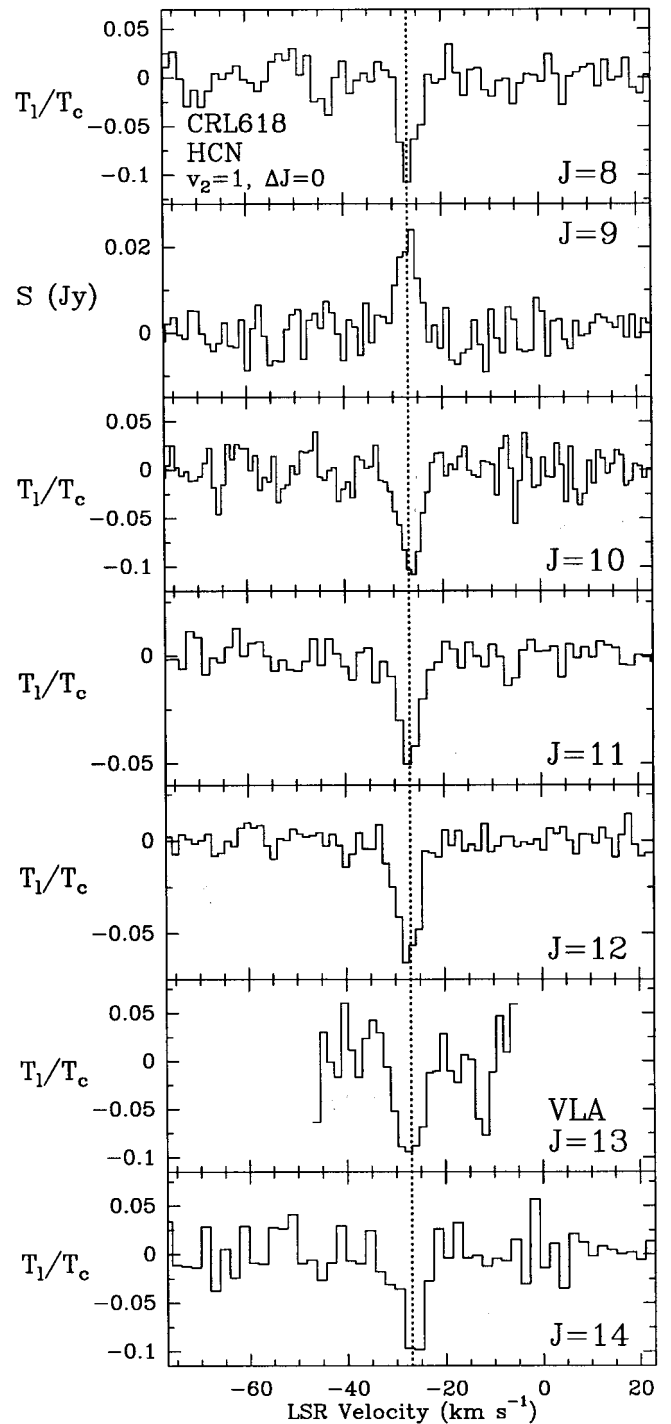

Fig. 2.—The $J = 8$, 9, 10, 11, 12, 13, and 14 $\Delta J = 0$ (direct l-type) transitions detected toward CRL 618. The $J = 8$, 9, 10, 11, 12, and 14 transitions were detected using the 100 m telescope, and the $J = 13$ transition using the VLA. The dashed line marks the line velocity $v_L = -27$ km s^{-1}, indicating a significant blueshift from $v_{sys} = -24.2$ km s^{-1} of CRL 618.

other spectra the ratio of line to continuum temperature, which reduces calibration uncertainties, is shown. The deviation of the HCN $J = 4$–3 model from the observed spectrum could be due to pointing and/or focus errors: a pointing error of $10''$ alone would explain the difference between observation and model and cannot be excluded. The model consists of power laws for temperature, density, and velocity starting at an inner radius of $0''\!.11$ and an H II
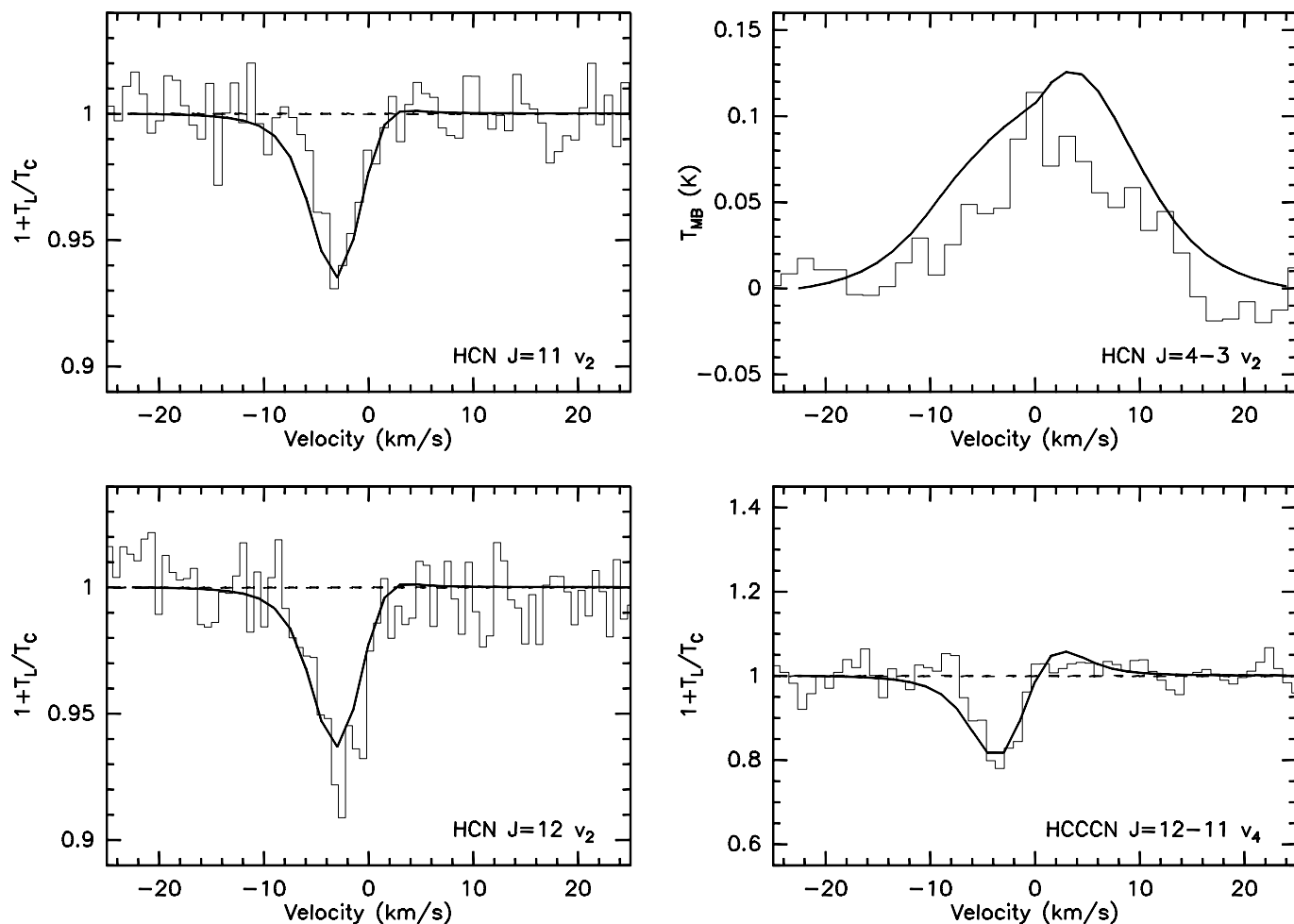
Fɪɢ. 3.—Comparison of observed spectra of vibrationally excited HCN/HC$_3$N with results of an expanding envelope model

region within that radius, which fits the continuum measurements of CRL 618. The temperature at the inner radius is 560 K. In the model, the HCN $J = 4$–3 line is highly optically thick and mostly sensitive to the model temperature and the emitting size. The HCN direct *l*-type lines, on the other hand, are optically thin and probe a combination of temperature and column density of the model. The best-fit model has an HCN/HC$_3$N abundance ratio of 3–6, depending on the assumed population of the vibrational levels of HC$_3$N, which is consistent with the result obtained with mid-infrared absorption measurements by Cernicharo et al. (2001).

Figure 4 shows the results of the VLA observations. The total continuum flux density at 40 GHz, estimated from the flux on the shortest baselines, is 0.75 Jy, with an uncertainty of 10%. The size of the continuum emission is $0.''34 \times 0.''16$, estimated from a Gaussian fit to the UV data. To increase the spectral sensitivity, every four channels were averaged together and a taper in the UV plane was applied, reducing the angular resolution to $0.''34 \times 0.''31$. The insert in Figure 4 shows the spectrum integrated over the indicated area. Line parameters of a Gaussian fit to the spectrum are given in Table 1. To image the HCN absorption, the continuum was subtracted from the data using the channel ranges marked in the insert of Figure 4. The contours in Figure 4 show the HCN absorption averaged over the line.

The observed 40 GHz continuum emission compares well with the results of Martín-Pintado et al. (1993, 1995) at 23 GHz. The HCN absorption falls into the same velocity range as the hot core (HC) component seen in ammonia by Martín-Pintado & Bachiller (1992). The HCN absorption is slightly shifted to the west from the center of the continuum, which was also seen for the HC ammonia component and the hot dense disk observed by Martín-Pintado et al. (1995). However, no absorption is observed at the ammonia broad absorption velocity of -50 km s^{-1}, which Martín-Pintado et al. (1993, 1995) interpreted as occurring from postshock clumps. Accordingly, the HCN absorption most likely originates from the same volume of gas as the ammonia HC component and the dense disk.

3.1. *A Weak J = 9 Maser?*

In contrast to the $J = 8$, 10, 11, 12, 13, and 14 transitions appearing as absorption lines toward the continuum, the $J = 9$ transition is found in emission. Blending with an unknown line cannot be ruled out entirely, but to the best of our knowledge there is no known transition of a different molecule, and no trace of a $J = 9$ absorption (which would modify the emission profile of the blending line) is seen. Moreover, the (blueshifted) velocity and the line width correspond well to the velocities and
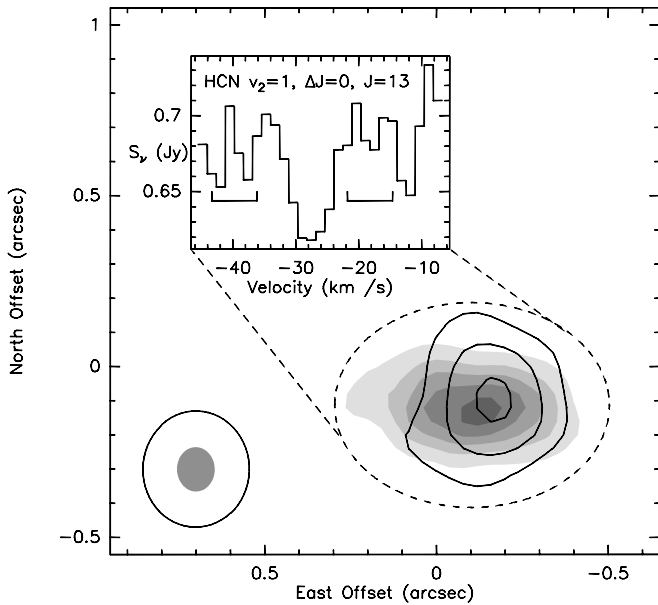
FIG. 4.—Results of the Q-band VLA observations. The continuum emission is shown in gray scale with steps of 10%, 30%, 50%, 70%, and 90% of the peak continuum flux (140 mJy beam^{-1}). The HCN absorption is shown in contours of -16.5, -27.5, and -38.5 mJy beam^{-1}, averaged from $V_{lsr} = -24.7$ to -30.3 km s^{-1}. The beam sizes are indicated on the lower left and are 0″13 × 0″11 and 0″34 × 0″31, respectively. The insert on the upper left shows a spectrum of the emission integrated over the region within the dashed ellipse.

line widths of the $J = 8$, 10, 11, 12, 13, and 14 transitions. In particular, the line width argument is compelling, since other emission lines are much broader (e.g., the line width of the HC$_7$N $J = 21$–20 transition is 27 km s^{-1}; Martín-Pintado & Bachiller 1992). These facts suggest that the $J = 9$ transition is a weak maser amplifying the continuum. Its optical depth has a different sign but is similar in value to the absorption lines.

How can this maser be understood? A quantitative analysis would require quite detailed modeling of the pumping mechanism, which is not feasible because many of the transition rates (in particular, collision rates between vibrational states and within the vibrationally excited state) are not or only poorly known. However, one can argue as follows that this transition is easily perturbed or inverted: the splitting due to l-type doubling is much smaller than the rotational splitting. Considering the rotational level system $J = 8$, $J = 9$ and assuming that the excitation temperature of the $J = 9e$–$8e$ is $T_{ex}^{9e,8e}$ (and equal to $T_{ex}^{8f,8e}$), while the excitation temperature for the f (upper) states is taken to be $T_{ex}^{9f,8f} = T_{ex}^{9e,8e} + \Delta T$ (with $\Delta T \ll T_{ex}^{9e,8e}$), one can show that inversion occurs ($T_{ex}^{9f,9e} < 0$) if the following condition is met:

$$\Delta T > \frac{\nu_{9f,9e}}{\nu_{8f,8e}} T_{ex}^{9e,8e} = 0.025 T_{ex}^{9e,8e} \; . \qquad (1)$$

In terms of occupation numbers, a difference $\Delta T = 2.5\%$ means that for an excitation temperature of 560 K, the occupation of the $J = 9f$ level needs to be elevated in population by only 0.17% with respect to a completely thermalized distribution to invert the direct l-type transition. If one considers the populations relative to the vibrational ground state, similar arguments can be made. A similar system is the

ammonia molecule, where the inversion splitting is much smaller than the rotational splitting, and indeed, some masers are found for ammonia as well (see Schilke, Walmsley, & Mauersberger 1991; Madden et al. 1986). It has to be emphasized that the actual pumping mechanism is probably quite different for the ammonia masers; the similarity is that it is not difficult to produce masers in the inversion lines.

Having argued that a small perturbation is sufficient, we still have to identify a possible cause for perturbations in our l-type system. One good candidate is a line overlap. Such a mechanism has been invoked successfully for pumping of OH masers (e.g., Cesaroni & Walmsley 1991), although the details of the pumping mechanism are different. One possible candidate responsible for a perturbation in the $J = 8$ and 9 $v_2 = 1$ levels is an overlap of rotational lines of the vibrationally excited molecule: for the $J = 8$–7 and $J = 9$–8 transitions of the $v_2 = 1$ and $v_2 = 2$ states, the l-components 1f and 2e are separated by only 11 and 58 MHz,[7] respectively, corresponding to $\Delta v = 5$ and 22 km s^{-1}. Accordingly, the first overlap could occur locally, whereas the second one could connect different parts of the envelope. A corresponding maser effect has been observed for SiO masers by Cernicharo, Bujarrabal, & Lucas (1991) and Cernicharo, Bujarrabal, & Santarén (1993).

3.2. HCN Direct l-Type Transitions in High-Mass Star-forming Regions

Initiated by the results presented here, additional searches for direct l-type transitions of HCN have been performed toward high-mass star-forming regions. So far, we have been able to detect the $J = 9$ transition toward Orion KL and Sgr B2(N) and the $J = 9$ and 10 transitions toward G10.47+0.03 using the Effelsberg 100 m telescope (S. Thorwirth et al. 2003, in preparation). Direct l-type transitions are optically thin and hence can be used to derive reliable column density estimates of the hot gas component. Moreover, the VLA observations of CRL 618 presented here demonstrate that this special kind of transition can be used to observe hot gas at high angular resolution and low frequencies.

4. SUMMARY

Using the Effelsberg 100 m telescope and the VLA, we have detected seven direct l-type transitions of HCN in its $v_2 = 1$ state. All lines appear in absorption against the embedded H II region, except for the $J = 9$ transition, which shows weak maser action. The observed line velocities agree well with those observed in vibrationally excited HC$_3$N by Wyrowski et al. (2003), who used their extensive data to model the physical parameters of the hot, dense emission region. VLA observations of the $J = 13$ line reveal that the emission region is compact and covers only the western part of the embedded H II region, similarly to ammonia. Since in addition to CRL 618 we detected l-type HCN lines toward hot molecular cores in regions of high-mass star formation, they also represent an interesting new tool for studying the immediate vicinity of young (proto)stellar objects.

[7] $J = 8$–7, $v_2 = 2$, $l = 2e$ at 712,361 MHz; $J = 8$–7, $v_2 = 1$, $l = 1f$ at 712,372 MHz; $J = 9$–8, $v_2 = 2$, $l = 2e$ at 801,421 MHz; and $J = 9$–8, $v_2 = 1$, $l = 1f$ at 801,363 MHz.

Triggered by the radio astronomical observations presented here, a laboratory investigation of direct l-type transitions of HCN ($v_2 = 1$) has been carried out in the Cologne laboratory covering rotational quantum numbers up to $J = 35$ at 278.7 GHz (Thorwirth et al. 2003). The complete analysis will be presented in a following paper.

REFERENCES

Brown, J. M., et al. 1975, J. Mol. Spectrosc., 55, 500
Cernicharo, J., Bujarrabal, V., & Lucas, R. 1991, A&A, 249, L27
Cernicharo, J., Bujarrabal, V., & Santarén, J. L. 1993, ApJ, 407, L33
Cernicharo, J., Heras, A. M., Tielens, A. G. G. M., Pardo, J. R., Herpin, F., Guelin, M., & Waters, L. B. F. M. 2001, ApJ, 546, L123
Cernicharo, J., et al. 1996, A&A, 315, L201
Cesaroni, R., & Walmsley, C. M. 1991, A&A, 241, 537
Madden, S. C., Irvine, W. M., Matthews, H. E., Brown, R. D., & Godfrey, P. D. 1986, ApJ, 300, L79
Maki, A. G. 1974, J. Phys. Chem. Ref. Data, 3, 221
Martín-Pintado, J., & Bachiller, R. 1992, ApJ, 391, L93
Martín-Pintado, J., Gaume, R., Bachiller, R., & Johnston, K. 1993, ApJ, 419, 725
Martín-Pintado, J., Gaume, R. A., Johnston, K. J., & Bachiller, R. 1995, ApJ, 446, 687
Menten, K. M., & Young, K. 1995, ApJ, 450, L67

Ott, M., Witzel, A., Quirrenbach, A., Krichbaum, T. P., Standke, K. J., Schalinski, C. J., & Hummel, C. A. 1994, A&A, 284, 331
Schilke, P., Güsten, R., Schulz, A., Serabyn, E., & Walmsley, C. M. 1992, A&A, 261, L5
Schilke, P., Mehringer, D. M., & Menten, K. M. 2000, ApJ, 528, L37
Schilke, P., & Menten, K. M. 2003, ApJ, 583, 446
Schilke, P., Walmsley, C. M., & Mauersberger, R. 1991, A&A, 247, 516
Shulman, R. G., & Townes, C. H. 1950, Phys. Rev., 77, 421
Thorwirth, S. 2001, Ph.D. thesis, Univ. Köln
Thorwirth, S., Müller, H. S. P., Lewen, F., Brünken, S., Ahrens, V., & Winnewisser, G. 2003, ApJ, submitted
Wyrowski, F., Schilke, P., Thorwirth, S., Menten, K. M., & Winnewisser, G. 2003, ApJ, 586, 343
Wyrowski, F., Schilke, P., & Walmsley, C. M. 1999, A&A, 341, 882
Ziurys, L. M., & Turner, B. E. 1986, ApJ, 300, L19